Journal of Chemical Neuroanatomy 38 (2009) 106–116

Contents lists available at ScienceDirect

Journal of Chemical Neuroanatomy

journal homepage: www.elsevier.com/locate/jchemneu

Regional and laminar distribution of the vesicular glutamate transporter, VGluT2, in the macaque monkey auditory cortex

Troy A. Hackett *, Lisa A. de la Mothe

Vanderbilt University School of Medicine, Department of Hearing and Speech Sciences, United States

ARTICLE INFO

Article history:
Received 20 January 2009
Received in revised form 4 May 2009
Accepted 5 May 2009
Available online 14 May 2009

Keywords:
Chemoarchitecture
Glutamatergic
Thalamocortical
Primate
Neuroanatomy
Connections

ABSTRACT

The auditory cortex of primates contains 13 areas distributed among 3 hierarchically connected regions: core, belt, and parabelt. Thalamocortical inputs arise in parallel from four divisions of the medial geniculate complex (MGC), which have regionally distinct projection patterns. These inputs terminate in layers IIIb and/or IV, and are assumed to be glutamatergic, although this has not been verified. In the present study, immunoreactivity (-ir) for the vesicular glutamate transporter, VGluT2, was used to estimate the regional and laminar distribution of the glutamatergic thalamocortical projection in the macaque auditory cortex. Coronal sections containing auditory cortex were processed for VGluT2 and other markers concentrated in the thalamorecipient layers: cytochrome oxidase, acetylcholinesterase, and parvalbumin. Marker expression was studied with wide field and confocal microscopy. The main findings were: (1) VGluT2-ir was highest in the core, intermediate in the belt, and sparse in the parabelt; (2) VGluT2-ir was concentrated in the neuropil of layers IIIb/IV in the core and layer IIIb in the belt; (3) VGluT2-ir matched regional and laminar expression of the other chemoarchitectonic markers. The results indicate that the glutamatergic thalamic projection to auditory cortex, as indexed by VGluT2-ir, varies along the core–belt–parabelt axis in a manner that matches the gradients of other markers. These chemoarchitectonic features are likely to subserve regional differences in neuronal activity between regions of auditory cortex.

1. Introduction

The auditory cortex of primates contains 13 areas distributed among 3 regions: core, belt, and parabelt (Hackett, 2007a; Kaas and Hackett, 2000) (Fig. 1A). The regions are interconnected in a manner consistent with a three-tiered processing hierarchy, where information appears to flow from the core to the belt, then on to the parabelt (Fig. 1B). In addition to cortical connection patterns, the division of auditory cortex into regions is supported by additional anatomical features.

First, each region of primate auditory cortex receives a different blend of inputs from the four major divisions of the medial geniculate complex (MGC) (de la Mothe et al., 2006b; Hackett et al., 1998b, 2007; Jones, 2007; Molinari et al., 1995; Morel and Kaas, 1992; Morel et al., 1993) (Fig. 1B). The main inputs to the core region arise from the tonotopically organized ventral division (MGv), which is an extension of the primary subcortical pathway. The belt region mainly receives inputs from the posterodorsal (MGpd) and anterodorsal (MGad) subdivisions of the dorsal division (MGd). The parabelt region receives mainly MGpd inputs, fewer inputs from the MGad no clear inputs from the MGv. All three regions receive inputs from the magnocellular, or medial, division (MGm).

Second, the chemoarchitecture of auditory cortex varies by region. The most robust feature is that the neuropil of the main thalamorecipient layers (IIIb and IV) stains darkly for several markers: acetylcholinesterase (AChE), cytochrome oxidase (CO) and parvalbumin (PV) (de la Mothe et al., 2006a; Hackett et al., 1998a, 2001; Jones, 2003; Jones et al., 1995; Morel and Kaas, 1992; Morel et al., 1993). Marker expression in the layer IIIb/IV band is greatest in the core, intermediate in the belt, and weakest in the

Abbreviations: A1, auditory area 1 (core); AChE, acetylcholinesterase; AL, anterolateral area (belt); CB, calbindin; CL, caudolateral area (belt); CM, caudomedial area (belt); CO, cytochrome oxidase; CPB, caudal parabelt area (parabelt); CS, central sulcus; Ins, insula; IPS, intraparietal sulcus; LGN, lateral geniculate nucleus; LS, lateral sulcus; LuS, lunate sulcus; MGad, medial geniculate complex, anterodorsal division; MGC, medial geniculate complex; MGd, medial geniculate complex, dorsal division; MGm, medial geniculate complex, magnocellular division; MGpd, medial geniculate complex, posterodorsal division; MGv, medial geniculate complex, ventral division; ML, middle lateral area (belt); MM, middle medial area (belt); Pro, proisocortical area; proA, prokoniocortex area; PS, principal sulcus; PV, parvalbumin; R, rostral area (core); Ri, retroinsular area; RM, rostromedial area (belt); RPB, rostral parabelt area (parabelt); RT, rostrotemporal area (core); RTL, rostrotemporal lateral area (belt); RTM, rostrotemporal medial area (belt); STG, supeior temporal gyrus; Tpt, temporal parietotemporal area; VGluT, vesicular glutamate transporter; VP, ventroposterior nucleus.

* Corresponding author at: Vanderbilt University, Department of Hearing and Speech Sciences, 301 Wilson Hall, 111 21st Avenue South, Nashville, TN 37203, United States. Tel.: +1 615 322 7491.
E-mail address: troy.a.hackett@vanderbilt.edu (T.A. Hackett).

0891-0618/$ – see front matter © 2009 Elsevier B.V. All rights reserved.
doi:10.1016/j.jchemneu.2009.05.002

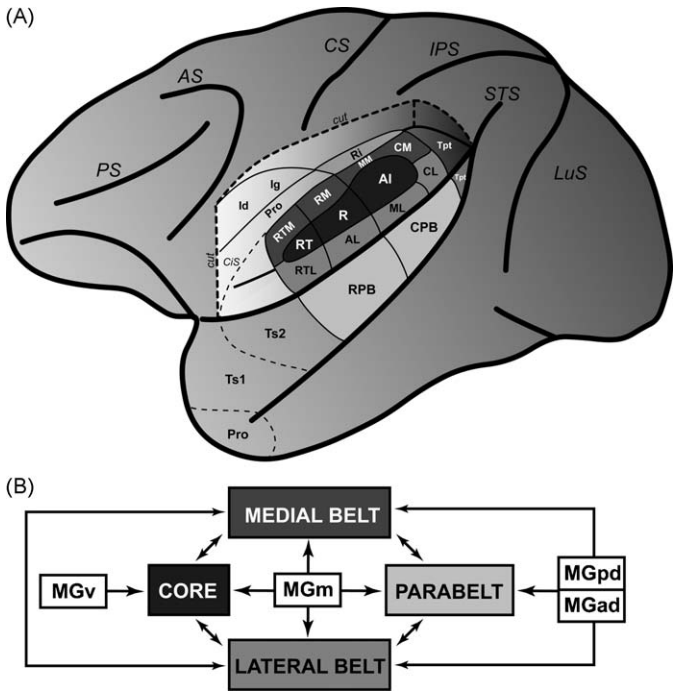

Fig. 1. Schematic diagrams of auditory cortex organization in the macaque monkey. (A) Left hemisphere with a portion of the parietal cortex removed graphically to show the location of auditory and auditory-related areas on the lower bank of the lateral sulcus (LS). Areas in the core region (A1, R, and RT); medial belt region (MM, CM, RM, and RTM); lateral belt region (CL, ML, AL, and RTL); parabelt region (CPB and RPB). (B) Major patterns of thalamocortical and corticocortical connections between the four major divisions of the medial geniculate complex (MGv, MGad, MGpd, and MGm) and regions of auditory cortex, color-coded as in panel (A). See the list of abbreviations for definitions, and text for other details about these connection patterns.

parabelt region. This density gradient reflects progressive reductions in both staining density and width of the IIIb/IV band along the core–belt–parabelt axis. Although the functional significance of these anatomical gradients is not well understood, it is reasonable to suppose that they contribute to activity-related differences between regions.

Considered together, thalamocortical input patterns and chemoarchitectonic marker distribution tend to covary along the core–belt–parabelt axis. Systematic decreases in layer IIIb/IV marker density are accompanied by shifts in the origin and laminar distribution of thalamic and cortical inputs, suggesting that these anatomical gradients are functionally linked. On the assumption that such gradients reflect activity-related differences between regions, we were led to consider whether there may also be gradients in the distribution of glutamatergic inputs along the core–belt–parabelt axis. Glutamate is widely assumed to be the principal excitatory neurotransmitter in cortex, and is well established as the primary excitatory neurotransmitter released by thalamocortical afferents in the auditory cortex (Cruikshank et al., 2002; Kharazia and Weinberg, 1994; LeDoux and Farb, 1991; Popowits et al., 1988). Accordingly, glutamatergic thalamocortical terminals should be concentrated in the IIIb/IV band, and in a manner that reflects the sublaminar projection patterns of each MGC division.

As an index of this feature, widefield and confocal microscopy were combined to study immunohistochemical expression of the vesicular glutamate transporter, VGluT2, in the macaque monkey auditory cortex. Vesicular glutamate transporters (VGluTs) regulate glutamate storage and release in synaptic vesicles (Fremeau et al., 2004a,b; Kaneko and Fujiyama; Kaneko et al., 2002b). The mRNA of the VGLuT1 and VGLuT2 isoforms are widely expressed by glutamatergic neurons in the spinal cord, brainstem, thalamus and cortex, although expression patterns vary between structures (Fremeau et al., 2004a, 2001; Hur and Zaborszky, 2005; Nahmani and Erisir, 2005). In some areas, VGluT1 and VGluT2 have been found in synapses with low and high-release probability, suggesting that the two transporters reflect distinct classes of glutamatergic projections with complementary distribution patterns and functional roles (Kaneko and Fujiyama, 2002a; Varoqui et al., 2002). In sensory systems, however, their segregation is not complete. In the primary somatosensory cortex (S1) of mice, Graziano et al. (2008) reported that the laminar distributions of VGLuT1 and VGluT2 immunoreactive terminals were partly overlapping. Specifically, VGluT2 immunoreactive (-ir) terminals were concentrated in layer IV, whereas VGluT1-ir terminals were concentrated in layers I–III, and less dense in layer IV. This pattern is comparable to other studies in which VGLuT2-ir was concentrated in layer IV terminals of visual and somatosensory cortex (Fujiyama et al., 2004; Kaneko et al., 2002b). Graziano et al. (2008) also found that both transporters were colocalized in many layer IV terminals. This appears to confirm an earlier observation in rats in which VGluT1 and VGluT2 mRNA were co-expressed in nearly all neurons in the primary sensory relay nuclei of the thalamus (Barroso-Chinea et al., 2007). In the MGC, VGluT1 mRNA expression was confined to the MGv, whereas neurons expressing VGluT2 were widely distributed in all divisions. In consideration of all of these findings, then, it appears that VGluT2-ir is a general marker of the glutamatergic thalamocortical projection to auditory cortex, whereas VGluT1-ir is associated both with corticocortical projections involving the supragranular layers, and the MGv projection to layer IV of A1 and perhaps other core areas.

2. Materials and methods

2.1. Tissue acquisition and histology

All procedures involving animals were conducted in accordance with international standards on animal welfare, followed NIH Guidelines for the Care and Use of Laboratory Animals, and were approved in advance by the Vanderbilt University Institutional Animal Care and Use Committee. Temporal lobes were obtained postmortem from two macaque monkeys (*M. radiata*). The animals were deeply anesthetized by a lethal dose of pentobarbital. Immediately after cardiac arrest the animal was perfused through the heart with 1 l each of the following solutions prepared in 0.1 M phosphate buffer (pH 7.4): 0.9% saline, cold (4 °C) 4% paraformaldehyde, and cold (4 °C) 4% paraformaldehyde plus 10% sucrose. Following perfusion the brains were removed and photographed. The cerebral hemispheres were separated from the thalamus and brainstem, blocked, and placed in 30% sucrose for 1–3 days. Blocks containing auditory cortex were cut frozen at 40 μm on a sliding microtome in an off-coronal plane, perpendicular to the long axis of the temporal lobe. Alternating series of sections were processed for Nissl (N) using thionin, acetylcholinesterase (AChE) (Geneser-Jensen and Blackstad, 1971), cytochrome oxidase (CO) (Wong-Riley, 1979), myelinated fibers (MF) (Gallyas, 1979), and immunohistochemistry for parvalbumin (PV), vesicular glutamate transporter 2 (VGluT2), and the neuron-specific protein, NeuN (details below). Some series were reacted for VGluT2 and PV or VGluT2 and NeuN using dual fluorescence immunohistochemistry.

2.2. Immunohistochemistry

In each animal, two to three adjacent series of sections were reserved for immunohistochemical detection of VGluT2, PV, and NeuN with monoclonal antibodies and fluorescent secondary antibody conjugates. All antibodies used are commercially available and have been well characterized (Table 1). Sections reserved for sequential double or triple-fluorescent immunohistochemistry were rinsed in 0.01 M phosphate buffered saline and 1% Triton X-100 (PBS-Tx) (pH 7.4), incubated for 2 h at room temperature in blocking solution (3% normal goat serum in 0.01 M PBS-Tx), then incubated for 48 h at 4 °C in blocking solution containing the primary antibody at the concentration listed in Table 1. After this incubation, sections were rinsed in PBS, then incubated for 24 h at 4 °C in a 1:200 solution of 0.01 M PBS containing one of three Alexa-fluor secondary anti-IgG conjugates (Invitrogen) (Table 1). Thereafter, sections were rinsed in PBS, and incubated in the second or third primary/secondary antibody combination. For each run, control sections not incubated in the primary antibody were reserved for comparison with reacted sections. Those comparisons revealed no cross-reactivity between antibodies. After completion of all incubations, sections were mounted on glass slides, coverslipped, and stored at 4 °C in the dark.

As an additional control, a separate series of sections was reacted for VGluT2 alone using the same primary antibody, but with a standard avidin–biotin complex